Edinburgh, Scotland
EURONOISE 2009
October 26-28

Prediction and auralization of construction site noise

Julien Maillard[1]
CSTB/Grenoble, 24 rue Joseph Fourier, 38400 Saint Martin d'Hères, France

ABSTRACT

This paper presents recent developments in auralization techniques applied to exterior noise assessment and control. The developments are part of an integrated software application that implements both the prediction and the auralization of construction site noise. The prediction of noise levels is based on a fast 2D beam tracer and standardized acoustic propagation models with added diffraction on vertical edges. The auralization module implements a real time restitution algorithm allowing user interactive navigation as well as source configuration. Three types of sources are supported: point sources, line sources and moving sources. The paper describes the signal processing methods used to obtain realistic and calibrated 3D audio rendering of the computed acoustic paths between sources and receiver. A special emphasis is placed on the treatment of path interpolation techniques during listener motion. The specific case of moving sources is also discussed.

1 INTRODUCTION

The perceptive evaluation of sound environments both indoors and outdoors has gained more interest with the developments of auralization techniques in the last few decades. Making acoustic simulation results "audible" adds another dimension to the analysis of the modeled sound fields, previously studied using numerical indicators only. Past research has shown the difficulty to evaluate the sound quality of a room or the performance of a noise control system based on sound pressure levels only. Auralization [1] brings a new analysis tool to study the characteristics of the sound environment, as perceived by a subject, under different configurations.

It should be clear that such perceptive evaluation is only valid for auralization systems able to render a close version of the real sound field. In addition, such systems often benefit from a certain level of user interaction in order to facilitate the study of the influence of physical parameters. Physical accuracy on one side and user interaction on the other side are two opposite constraints in terms of computational requirements and much research has been conducted to develop auralization systems that satisfy both constraints with limited computational resources [2, 3, 4]. Auralization generally implies the use of a physical model based on geometrical acoustics in order to separate the sound field into elementary plane or spherical wave contributions. These contributions can then be auralized using existing 3D sound restitution systems over headphones or loudspeakers. The main challenge is to compute and auralize the perceptively important contributions only such that the system runs in real time and therefore features some level of user interaction [5].

This paper presents recent developments in auralization techniques applied to the evaluation of exterior noise pollution. Most of the advanced research conducted so far in the field of auralization deals with closed acoustic spaces [6]. Closed volumes usually feature a complex sound field

[1] julien.maillard@cstb.fr

resulting from a large number of interactions with the geometry. Outdoor noise pollution can also greatly benefit from auralization systems. In this type of environments, the sound field is generally less reverberant than inside closed spaces. This potentially reduces the number of elementary contributions to auralize for a valid reproduction of the real sound field. On the other hand, outdoor noise is usually the result of a great number of independent sources, which can be moving in the case of traffic noise. The objective of this research is the physical based auralization of traffic noise, that is the auralization of a large number of moving sources. Unlike previous work in this field which used pre-recorded traffic noise processed in real time to match computed sound pressure levels at the listening point [7], the current system treats each moving source individually based on the model-driven acoustic emission and position parameters.

As a first step towards the auralization of complex traffic noise, the present work deals with a reduced number of moving sources such as large earth-moving equipments commonly found on construction site. It is part of a recently developed software application that implements the simulation and auralization of construction site noise. The application integrates the different steps required to analyze the noise exposure through listening tests: geometry modeling of the site under study, definition of noise sources and meteorological parameters, visual analysis of noise levels on an interactive 3D view of the site, and finally, interactive auralization of all modeled sources. This integrated application combines the quantitative analysis of construction site noise with the perceptive evaluation of its impact on workers and nearby populations. In addition to the optimization of the noise protections and machine operations, the first aspect can be used to verify the compliance with existing noise regulations while the second aspect might serve communication purposes during public briefings discussing noise annoyance [8].

The paper describes some of the signal processing methods and algorithms implemented in the audio rendering module of the application mentioned above. In particular, a number of techniques that are well suited to the auralization of outdoor noise and more specifically to the auralization of moving sources are discussed. After a brief overview of the auralization module, the following sections discuss specific aspects of the algorithms implemented in the module: the propagation path interpolation technique during listener motion, the propagation delay calculation considering the special case of moving sources, and the interpolation of delays.

2 OVERVIEW

The auralization system discussed in this paper is capable of rendering the sound field generated by a number of sources within a given outdoor geometry. The audio restitution is performed in real time and allows interactive listener motion over a 2D surface parallel to the ground terrain. The user can also change dynamically the emission properties of the sources. A visual interface provides an interactive 3D view of the scene under study, including colored maps that represent the sound pressure level calculated over the area of audio restitution.

The different modules of the application and their connections are shown on the diagram of Figure 1. The green modules are modified during real time auralization while the red modules are operating off-line and have read-only access otherwise. In the current implementation, the acoustic calculation is performed off-line. During this pre-processing stage, the transfer functions between each source and a map of receivers covering the listening area are calculated. Each transfer function contains a number of propagation paths. At most N of these propagation paths are kept individually and saved in the paths database. The additional paths of a source-receiver

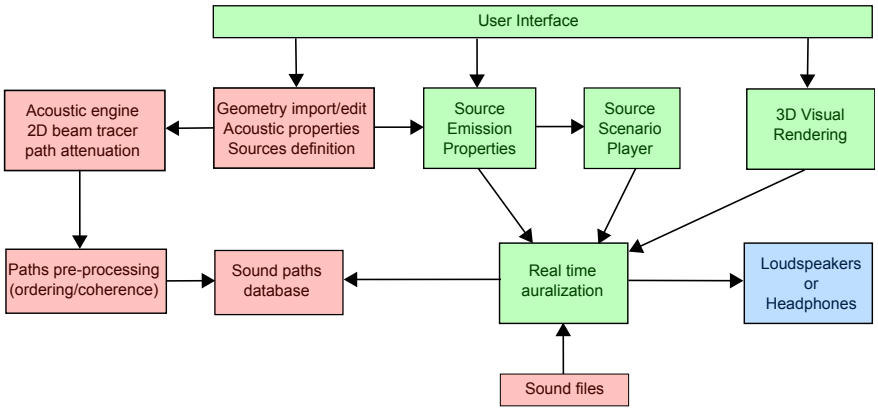

Figure 1: General architecture of the auralization system.

transfer function are combined into a single residual path as will be described below. During audio restitution, the auralization module accesses the paths database to update the appropriate signal processing nodes based on the current listening position. This approach was found appropriate for the current application due to the limited number of significant contributions in the type of environments under study as well as the relatively small number of sources. The chosen approach also allows the simultaneous display of a sound pressure map over the entire listening area. Future work will however consider the possibility of calculating in real time the propagation paths between sources and receivers near the listening point. The obvious benefit of a real time approach is the increase of the listening area which is currently limited by the amount of memory available as well as the ability to modify the site geometry during restitution.

The geometry and source definition module contains the complete model of the site under study, i.e., definition of terrain, building and sound protections, including acoustic surface impedance and definition of noise sources. This data can be imported and edited within the application. Three elementary source types are available: point source, line source, and moving point source. Each source is characterized by its geometry, its far-field directivity, its radiated acoustic power and its audio signature. For line sources, the geometry is defined by a multi-line made of 2 point segments. For moving sources, the geometry defines the trajectory of the source using the same multi-line segments.

For the present application, experimental characterization of various machines commonly found on construction site was performed in order to estimate the sound power level of equivalent point or line sources and their directivity. The audio signatures of the source under study were also recorded. Recording conditions were chosen such as to obtain a signal with good signal to noise ratio which is a close estimate of the acoustic pressure radiated in the far field under free field conditions. For moving point sources, specific treatments were implemented to generate the appropriate audio signature from a fixed recording position. Assuming constant speed and knowing the position of the moving source, the inversion of the Doppler effect yields a good representation of the source signature over a short time period. The obtained signal is then extended over a longer period using specifically developed time expansion algorithms.

The acoustic engine includes two separate modules: the path finder engine and the point-to-point acoustic engine. Together, these two modules implement standardized prediction methods for outdoor noise based on geometrical acoustics, namely the International ISO-9613 standard and the French NMPB-96 standard [9, 10]. The current implementation also takes into account diffraction

on vertical edges for specific buildings and protections. Future versions will implement the point-to-point formulation developed during the European Harmonoise project [11].

The path finder engine implements a 2D beam tracer in the horizontal plane. For the purpose of auralization, line sources and moving point sources are replaced in the acoustic engine by a set of point sources equally spaced along source line geometry. For line sources, this decomposition enables proper auralization of the source spatial extent. For moving point sources, the equivalent point sources are ordered along the source trajectory according to the direction of motion and associated with time instants based on the source speed. As described below, time interpolation of the sound paths is then implemented to recreate the time varying sound field associated with the moving source.

Once a propagation path has been identified by the path finder engine, its associated sound attenuation is calculated by the point-to-point acoustic engine, taking into account the vertical profile along the path, the reflections and diffractions on horizontal edges, as well as the meteorological effects. In the current implementation and following the ISO-9613 and NMPB-96 standards [9, 10], the acoustic properties of sources and materials are represented by statistical mean values in octave frequency bands between 63 and 8000 Hz. Each propagation path is therefore defined by 8 attenuation gains, a propagation delay based on the path distance and a direction of arrival. The summation in energy within each frequency band has been shown to be valid for broadband sources such as industrial and traffic noise. Construction site noise also enters this category.

The auralization module implements the 3D audio restitution of a number of image sources with appropriate propagation delay, direction of arrival and frequency dependent attenuation. Each one of these sources is associated with an audio signature and a propagation path. In cases where several propagation paths are saved in the pre-processing stage, the same audio signature may be shared by several propagation paths.

As mentioned earlier, for a 3D auralization of the sound field at the receiving point, the perceptively most important acoustic paths must be rendered individually in order to accurately reproduce the spatial properties of the sound field. To this purpose, the propagation paths are ordered according to their perceptive importance and saved individually in the paths database. Assuming the N most important paths are rendered individually, the contribution from the remaining paths is replaced by a single path with attenuation obtained by summing the attenuation of the original paths. The geometrical characteristics of this residual path (propagation distance and direction of arrival) are based on the most significant path among the remaining paths.

The perceptive ordering of paths should follow the principles of psychoacoustics and the different masking laws associated with the perception of 3D sound fields [12]. In the current implementation, the ordering is based solely on the geometrical spreading factor. Masking effects due to close time or direction of arrival are therefore neglected.

For efficient implementation, the audio signatures are pre-filtered and loaded into memory prior to restitution. The resulting 8 sub-band signal buffers are accessed by circular pointers to implement the fractional propagation delay of a single path. Each sub-band signal is then run through the frequency equalization gain and summed to obtain the properly attenuated signal. The resulting single channel signal is finally processed by the 3D rendering unit based on the current listener orientation and the associated path arrival direction. The 3D unit implements an efficient binaural restitution algorithm [13, 14] for headphone restitution. Restitution over speakers based on Vector-Based-Amplitude-Panning [15] is also available in the application. Figure 2 presents a schematic of the signal processing flow associated with a single propagation path. Note that for moving point

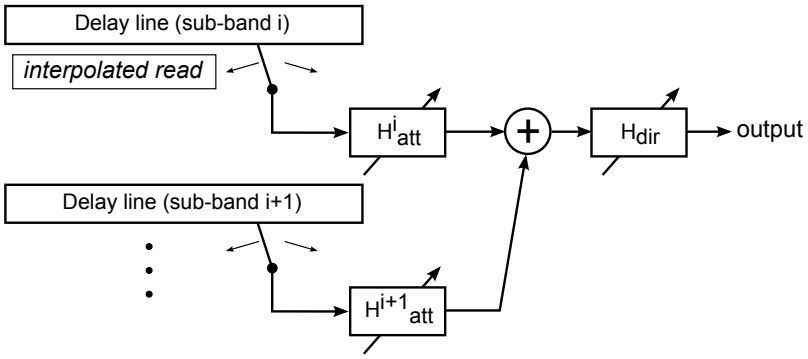

Figure 2: Signal processing block diagram associated with a single propagation path.

sources and during listener motion, some propagation paths will be interpolated in time as described later in this paper. Consequently, all delay, attenuation and directional processing units have varying parameters that are interpolated on a sample base to avoid audible artifacts.

3 PROPAGATION PATHS INTERPOLATION

As described above, the auralization system uses a database of pre-calculated propagation paths over a set of discrete receiver positions. Therefore, auralizing the sound field for any listener position requires paths interpolation.

Path interpolation takes place any time the listener is moving or in presence of a moving source. In both cases, the set of current active paths associated with the current listener and/or moving source position, the current set, must be replaced by a new set of paths associated with the next positions, the target set. Obviously, this transition must preserve path coherence. That is paths that are associated with the same image source must be interpolated. Current paths that do not have a coherent path in the target set are terminated and target paths that do not have a coherent path in the current set are started. This is illustrated in Figure 3. The figure shows 2 receiver positions,

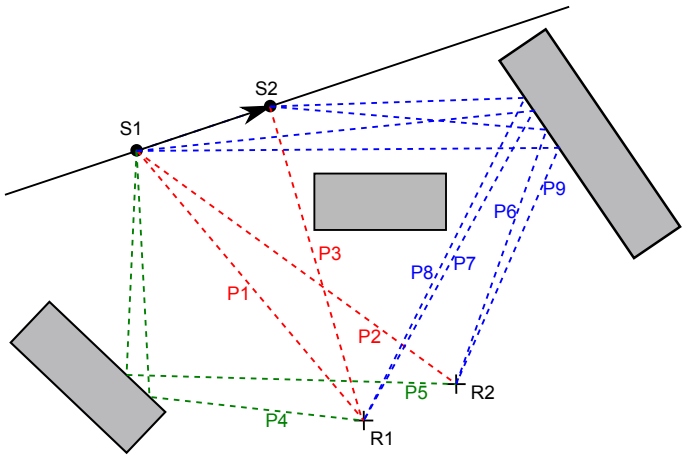

Figure 3: Schematic of coherent propagation paths identification.

R_1 and R_2, 2 source positions, S_1 and S_2, and 3 buildings. All specular propagation paths up to the first order of reflection are represented by dashed lines between the source and receiver positions. Coherent paths are drawn with the same color.

Let first consider the case where the listener moves from current position R_1 to the next position R_2 and S_1 and S_2 represent two independent point sources. Coherent paths are interpolated, i.e., P_1 is interpolated towards P_2, P_4 towards P_5, P_7 towards P_9, and so on. Path P_3 associated with source S_2 and receiver R_1 is terminated since it does not have a coherent path at receiver position R_2. Now consider the case where S_1 and S_2 represent two adjacent point sources along the trajectory of a moving source. If the listener remains fixed at receiver position $R1$, path P_1 is interpolated towards P_3, P_7 towards P_8, while path P_4 is terminated and path P_3 is started. Finally, if S_1 and S_2 represent two adjacent point sources and the listener moves from $R1$ to $R2$, then P_1 and P_4 are terminated, and P_7 is interpolated towards P_6.

The above interpolation approach requires the identification of all coherent paths. This path coherence information is built during a pre-processing stage (see Figure 1). For each propagation path between a source and receiver, the position of the associated image source is constructed based on the path distance and the direction of arrival at the receiver. For each point source, the set of image sources associated with all receivers is processed in order to find multiple image sources and identify coherent paths which are assigned a unique identification number. In the case of moving point sources, coherence must also be set between paths of 2 adjacent point sources along the source trajectory. Consider two adjacent equivalent point sources S_i and S_{i+1}. Each image source associated with S_i is translated by the corresponding image of the vector from S_i to S_{i+1}. This new position is then compared to the image sources associated with S_{i+1} in order to identify coherent paths.

Path interpolation is implemented at the signal processing level using sample base interpolation. As shown in Figure 2, each active propagation path is associated with 8 sub-band fractional delay lines, 8 attenuation gains and a direction of arrival relative to the listener's head orientation. The interpolation is performed by incrementing the delays, gains, and direction of arrival at each sample in order to reach a target value after a given number of samples. Note that the incremented parameters for the 3D audio rendering unit are internal gains and delays rather than actual direction angles, allowing to perform the conversion from angles to gain values only once at each new target update.

So far, the listener is assumed to move from one pre-calculated receiver to another. This assumption is only feasible if receivers are equally spaced over the listening area with a controlled mesh size. To allow arbitrary receiver locations and resolution, the auralization system must implement the restitution for any listener position. Each propagation path is associated with an image source position. Therefore the propagation delay and direction of arrival is easily updated for any listener position. The path attenuation gains however are only known at the receiver positions and must be interpolated at the current listener position. To this purpose, the three closest receivers around the listener position are selected each time the listener moves to a new position. The algorithm then considers coherent paths that are associated with all three receivers and interpolates gain values based on the gains of the three coherent paths and distances to the three receivers.

4 PROPAGATION DELAY AND DIRECTION OF ARRIVAL

The calculation of propagation delays and directions of arrival is now discussed considering the general case of a moving source and a moving receiver. A specific algorithm is implemented for moving sources in order to obtain a physically valid auralization. Figure 4 illustrates the propagation of a wave front from a moving source to a moving receiver. On the left, the source emits a wave

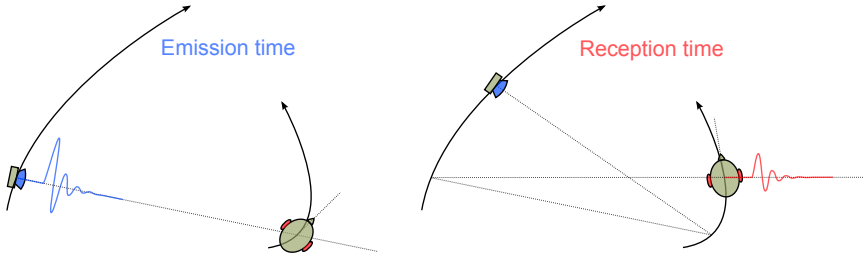

Figure 4: Wave-front propagation between a moving source and moving receiver.

front (blue signal) at emission time. On the right, the wave front (red signal) reaches the receiver at reception time t. Let $\mathbf{r_R}(t)$ and $\mathbf{r_S}(t)$ represent respectively the receiver and source position at time t. The propagation delay at reception time, $\tau(t)$, must satisfy the relation

$$|\mathbf{r_R}(t) - \mathbf{r_S}(t - \tau(t))| = c\tau(t) \tag{1}$$

where c represents the speed of sound. The frequency dependent attenuation at time t is based on the attenuation associated with the source position at emission time, $\mathbf{r_S}(t-\tau(t))$, and the receiver position at reception time, $\mathbf{r_R}(t)$. The direction of arrival $(\theta,\phi)(t)$ is based on the angle between the listener orientation at reception time, $\mathbf{r_H}(t)$ and the source-receiver vector $\mathbf{r_{RS}}(t) = \mathbf{r_S}(t-\tau(t)) - \mathbf{r_R}(t)$: $(\theta,\phi)(t) = \angle(\mathbf{r_H}(t), \mathbf{r_{RS}}(t))$.

An analytical solution to Eq. (1) can be obtained in the special case where the source moves along a straight line. In the present application, the source trajectory is discretized into a set of adjacent point sources which define straight line segments. Let $\mathbf{r_S^k}(t) = \mathbf{r_{0,S}^k} + \mathbf{v_S^k}(t-t_k)$, the source position at time t on segment k where $\mathbf{r_{0,S}^k}$ is the starting point of segment k and t_k is such that $\mathbf{r_S^k}(t_k) = \mathbf{r_{0,S}^k}$. Note that the line segments are also defined for image sources of coherent paths. Replacing $\mathbf{r_S^k}(t)$ in Eq. (1), the propagation delay associated with segment k is obtained as the root of a second order polynome [16]:

$$\tau^k(t) = \frac{1}{c^2 - \|\mathbf{v_S}\|^2}\left\{\left(\mathbf{r_R}(t) - \mathbf{r_{0,S}^k} - \mathbf{v_S}(t-t_k)\right)\cdot\mathbf{v_S} + \sqrt{\left(\left(\mathbf{r_R}(t) - \mathbf{r_{0,S}^k} - \mathbf{v_S}(t-t_k)\right)\cdot\mathbf{v_S}\right)^2 + \left\|\mathbf{r_R}(t) - \mathbf{r_{0,S}^k} - \mathbf{v_S}(t-t_k)\right\|^2\left(c^2 - \|\mathbf{v_S}\|^2\right)}\right\} \tag{2}$$

The algorithm starts by calculating the propagation delay for segment k such that $t_k \leq t < t_{k+1}$. If $\tau^k(t) \leq t - t_k$, the attenuation and direction of arrival are obtained from the source position, $\mathbf{r_S^k}(t - \tau^k(t)) = \mathbf{r_{0,S}^k} + \mathbf{v_S^k}(t - \tau^k(t) - t_k)$ and the current listener position. If not, the propagation is calculated for the previous segment $k-1$. This is repeated up to the first segment of the trajectory. If $\tau^k(t) \leq t - t_k$ is not verified for any source segment, the source wave front has not yet reached the receiver and no path is started. The above procedure is also performed for all image source segments. Once the source position at emission time, $\mathbf{r_S^k}(t-\tau^k(t))$ is obtained, the actual attenuation gains are calculated using a linear interpolation between the two propagation paths associated with source segment k. This procedure is performed at a constant time rate generally equal to a integer number of audio processing blocks.

The above method assumes the source speed is constant over each segment, i.e., zero accel-

eration. However, it is still possible to auralize a variable speed source motion since sample base interpolation is performed between each target update. Also note that an analytical solution can still be derived for constant acceleration. It is not clear however whether this would improve the quality of auralization.

5 DELAY INTERPOLATION

Recalling the block diagram of Figure 2, the delay associated with a propagation path is implemented using a circular buffer and variable read-access pointers. As discussed in the previous section, coherent paths are interpolated during listener motion or in presence of moving sources. Consequently, the delay line implements a fractional delay whose value is updated every sample. This approach ensures smooth phase transitions and no audible artifacts. The current implementation uses a fractional delay based on a first order Lagrange interpolator [17, 18].

The variable propagation delay calculated according to the methods presented in the previous section introduces a physical based Doppler effect. In other word, the variable delay causes a frequency modulation or Doppler shift which can be expressed as $1 - d\tau(t)/dt$. It follows that interpolating the propagation delay between two target updates using linear interpolation will produce a constant Doppler shift, since the delay derivative is then equal to the constant delay increment. Every time the delay target is updated, the linear interpolation sets the delay increment to a new value which in turn generates a sudden change in Doppler shift. This artificial effect is clearly audible when auralizing a pure tone passing by the listener.

To eliminate the above discontinuous Doppler shift, it was decided to implement a cubic interpolation for the propagation delay values. As shown below, cubic interpolation guaranties the continuity of the delay derivative and therefore produces a continuous frequency modulation which is consistent with the perception of real sources. Cubic interpolation represents the variable delay $\tau(t)$ as an order 3 polynomial expression. The coefficients of the polynome are calculated based on the delay value and its first derivative at the previous and next target update times t_k and t_{k+1}. Recalling the notations from the previous section, the delay derivative is obtained at time t by deriving the expression $\tau(t) = |\mathbf{r_R}(t) - \mathbf{r_S}(t - \tau(t))|/c$. The resulting expression gives the delay derivative in terms of the receiver position and speed, respectively $\mathbf{r_R}(t)$ and $\mathbf{v_R}(t) = d\mathbf{r_R}(t)/dt$, and the source position and speed at emission time $t - \tau(t)$, respectively $\mathbf{r_S}(t - \tau(t))$ and $\mathbf{v_S}(t - \tau(t)) = d\mathbf{r_S}(t - \tau(t))/dt$:

$$\frac{d\tau}{dt}(t) = 1 - \left(1 - \frac{(\mathbf{r_R}(t) - \mathbf{r_S}(t - \tau(t))) \cdot \mathbf{v_R}(t)}{|\mathbf{r_R}(t) - \mathbf{r_S}(t - \tau(t))|\, c}\right) \Big/ \left(1 - \frac{(\mathbf{r_R}(t) - \mathbf{r_S}(t - \tau(t))) \cdot \mathbf{v_S}(t - \tau(t))}{|\mathbf{r_R}(t) - \mathbf{r_S}(t - \tau(t))|\, c}\right) \quad (3)$$

Rather than evaluating the order 3 polynomial expression upon every sample, a more efficient discrete recursive formulation is now proposed to obtain the interpolated delay values. Let x_i represent the delay value at discrete time i. For a cubic interpolation, and assuming a constant sampling rate, the delay value verify the following recursive formulation:

$$z_i = z_{i-1} + \beta \qquad y_i = y_{i-1} + z_{i-1} \qquad x_i = x_{i-1} + y_{i-1} \quad (4)$$

where β is a constant value. Assuming the delay is interpolated between discrete time i_k and i_{k+1}, the problem must solve for z_{i_k} and β knowing the delay and its derivative at the two end points, i.e.,

$$x_{i_k} = X_k \qquad x_{i_{k+1}} = X_{k+1} \qquad y_{i_k} = Y_k \qquad y_{i_{k+1}} = Y_{k+1} \quad (5)$$

After developing the recurrence formula given above and solving the resulting linear system, the solution for z_{i_k} and β is expressed as

$$z_{i_k} = (Y_{k+1} - Y_k)\frac{-2(M-2)}{M(M+1)} + (X_{k+1} - X_k - MY_k)\frac{6}{M(M+1)} \quad (6)$$

$$\beta = (X_{k+1} - X_k - MY_k)\frac{-12}{M(M-1)(M+1)} + (Y_{k+1} - Y_k)\frac{6}{M(M+1)} \quad (7)$$

where $M = i_{k+1} - i_k$. Note that M must not be too large in order to avoid numerical errors.

To illustrate the influence of propagation delay interpolation, the auralization system presented in this paper was run on a simple test case based on a single moving source with a pure tone signature. The listener was located at the coordinate origin and facing the x-axis direction. The source trajectory was defined by point sources along a line parallel to the y-axis starting at coordinate $(-80\,\text{m}, 15\,\text{m})$ and moving in the direction of increasing y coordinates at a speed to $40\,\text{m/s}$. Adjacent equivalent point sources are $40\,\text{m}$ apart. The sampling frequency was $44100\,\text{Hz}$ and the target update was performed every 8196 samples. During restitution, the target delay value and its first derivative, X_k and Y_k, were logged to a file upon every target update. The interpolated delay value x_i set in the fractional delay line were also logged at every sample. This test case was performed twice using linear and cubic delay interpolation. Post-processing calculated the interpolated delay increment in both cases.

Figure 5 shows the propagation delay and its derivative during source pass-by motion for both test cases described above. The solid and dashed lines represent linear and cubic interpolation,

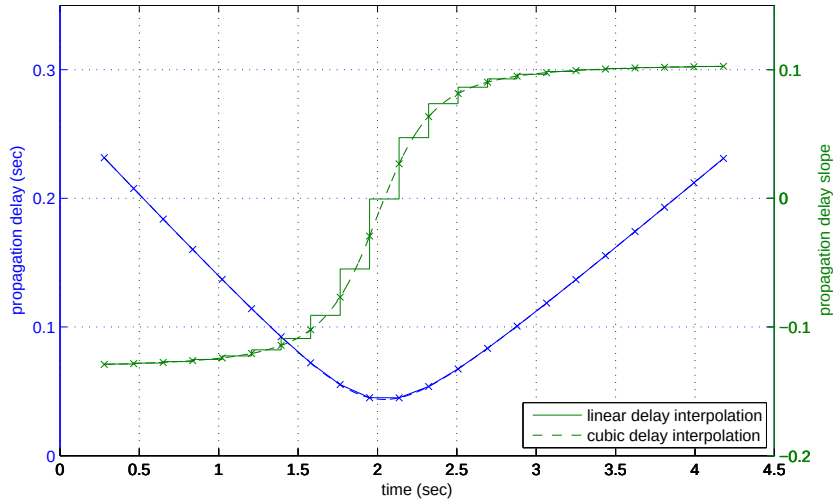

Figure 5: Propagation delay and its derivative for a moving source using linear interpolation (solid lines) and cubic interpolation (dashed lines).

respectively. The x-marks show the target values for the delay and its derivative. Examining the blue curves, the interpolated delay strictly follows the target values as expected both for the linear and cubic interpolation, which validates the formulation presented here. The delay increment plotted in green represents the delay derivative. As expected, the increment matches the target values for the cubic interpolation. Furthermore, the solid line associated with the linear interpolation clearly shows discontinuities at each target update which results in audible discontinuous variations of the Doppler shift. While these variations are small when the source is far away, they become clearly

audible around the passage point. On the other hand, cubic interpolation (dashed green line) yields a smooth continuous Doppler shift.

6 CONCLUSIONS AND PERSPECTIVES

The methods and algorithms presented in this paper allow the auralization of outdoor noise sources over extended listening areas. The auralization approach uses a physical model of the sound propagation between sources and a set of receivers based on geometrical acoustics. Fixed and moving point sources as well as line sources are auralized in real time using multiple path contributions. The user is able to move freely over the restitution area as well as modify dynamically the sources emission properties. The propagation path interpolation technique during source and listener motion is presented. A physically valid algorithm is also described for the calculation and rendering of accurate propagation delays and time varying spatial directions in the general case of moving sources and moving listener. Finally, a cubic interpolation approach is introduced for setting the propagation delay in order to eliminate audible discontinuous Doppler shifts.

Future work will further optimize the proposed algorithms to support an increased number of moving sources and provide an auralization system for traffic noise based on individual vehicle restitution. The system will be coupled to a traffic model which provides in real time vehicle position and speed at regular intervals based on current traffic global parameters. This work will also include recent progress in source signal generation for variable speed vehicles.

7 REFERENCES

[1] M. Kleiner, B. I. Dalenbäck, and P. Svensson, "Auralization - An overview", Journal of the Audio Engineering Society **41**, 861–875 (1993).

[2] T. Funkhouser, N. Tsingos, I. Carlbom, G. Elko, M. Sondhi, J. E. West, G. Pingali, P. Min, and A. Ngan, "A beam tracing method for interactive architectural acoustics", The Journal of the Acoustical Society of America **115**, 739–756 (2004).

[3] A. Silzle, P. Novo, and H. Strauss, "IKA-SIM: A system to generate auditory virtual environments", in *Audio Engineering Society-116th Convention May 8-11 Berlin, Germany* (2004).

[4] S. Laine, S. Siltanen, T. Lokki, and L. Savioja, "Accelerated beam tracing algorithm", Applied Acoustics **70**, 172 – 181 (2009).

[5] R. Kajastila, S. Siltanen, P. Lundén, T. Lokki, and L. Savioja, "A distributed real-time virtual acoustic rendering system for dynamic geometries", in *122nd AES Convention, Vienna, Austria*, Convention Paper 7160 (2007).

[6] P. Svensson and U. R. Kristiansen, "Computational modelling and simulation of acoutic spaces", in *22nd International AES Conference, Helsinki, Finland*, Paper 266 (2002).

[7] J. Maillard and J. Martin, "A simulation and restitution technique for the perceptive evaluation of road traffic noise", in *ForumAcusticum 2005, Budapest* (2005).

[8] P. Autuori, M. Cottet, and M. Aubrit-Clochard, "Noise from construction sites: a new software for acoustic simulation and restitution", in *16th International Congress on Sound and Vibration, Krakow, Poland* (2009).

[9] J. Defrance and Y. Gabillet, "A new analytical method for the calculation of outdoor noise propagation", Applied acoustics **57**, 109–127 (1999).

[10] J. Defrance, M. Bérengier, and J. Rondeau, "Validation and evolution of the road traffic noise prediction method NMPB-96. Part 2: Improvements based on theoretical models", in *Inter-Noise'2001, Den Haag, The Netherlands* (2001).

[11] D. van Maercke and J. Defrance, "Development of an analytical model for outdoor sound propagation within the harmonoise project", Acta Acustica united with Acustica **93**, 201–212 (2007).

[12] J. Blauert, *Spatial hearing, the psychophysics of human sound localisation* (MIT Press) (1997).

[13] M. Emerit, E. Dudouet, and J. Martin, "Head related transfer function and high order statistics", in *15th International Congress on Acoustics*, 437–440 (Trondheim, Norway) (1995).

[14] E. Dudouet and J. Martin, "A new HRTF decomposition and algorithm for sound spatialization", in *ASA/DAGA Joint Meeting, Berlin, 14-19 March* (1999).

[15] V. Pulkki, "Virtual sound source positioning using vector base amplitude panning", JAES **45(6)**, 456–466 (1997).

[16] H. Strauss, "Implementing doppler shifts for virtual auditory environments", in *Convention paper 4687, Presented at the 104th Convention 1998 May 16-19 Amsterdam*, edited by A. E. Society (1998).

[17] T. I. Laakso, V. Valimaki, M. Karjalainen, and U. K. Laine, "Splitting the unit delay [fir/all pass filters design]", **13**, 30–60 (1996).

[18] A. Franck, "Efficient algorithms and structures for fractional delay filtering based on lagrange interpolation", **56**, 1036–1056 (2008).